Slovak University of Technology in Bratislava
Institute of Information Engineering, Automation, and Mathematics

PROCEEDINGS

of the 18th International Conference on Process Control

Hotel Titris, Tatranská Lomnica, Slovakia, June 14 – 17, 2011

ISBN 978-80-227-3517-9

http://www.kirp.chtf.stuba.sk/pc11

Editors: M. Fikar and M. Kvasnica

Masar, I., Stöhr, E.: Gain-Scheduled LQR-Control for an Autonomous Airship, Editors: Fikar, M., Kvasnica, M., In *Proceedings of the 18th International Conference on Process Control*, Tatranská Lomnica, Slovakia, 197–204, 2011.

Full paper online: http://www.kirp.chtf.stuba.sk/pc11/data/abstracts/097.html

Gain-scheduled LQR-control for an autonomous airship

I. Masár and E. Stöhr *

* *FernUniversität in Hagen*
Process Control Engineering Group
Universitätsstr. 27
58093 Hagen, Germany
(Tel: +49 2331 9871102; e-mail: ivan.masar@fernuni-hagen.de)

Abstract: In the past two years, an autonomous airship was developed at our department as a flying sensor platform. Our main research areas during this period were navigation, modelling and automatic control of the airship. In this article, we present a gain-scheduled LQR control design for the airship. First, the mathematical model of the system and its linearization will be introduced. After that, we split the linearized system in a lateral and a longitudinal subsystem. With the combined gain-scheduled controlled subsystems, a high-level navigation system allows the airship to follow an appropriate flight trajectory.

Keywords: airship, LQR control, gain scheduling.

1. INTRODUCTION

Unmanned aerial vehicles (UAV's) became very popular in the last years, because of the availability of cheap HW components likes motors, sensors (digital gyroscopes, compass, accelerometers, barometers, etc.), embedded microcontrollers and power units. There exists plenty of designs, including autonomous helicopters and quad- (or more-) copters ([Prior et al. (2009)], [Jaimes et al. (2008)]), but they have a few common problems - typically a very small payload capacity, a short flight time and an intrinsic instability. These properties reduce the number of possible applications to short-time reconnaissance missions - very often with low-cost and therefore low-quality cameras.

As we were confronted with the problem of designing an UAV, which could be used as a carrying platform for a lot of various sensor and camera systems for a couple of hours, which should be safe for ground personal and easy to manoeuvre for the operator, we decided to return back to aviation roots and to design an autonomous airship. Namely, there are some very advantageous properties of such lighter-then-air flying system. In particularly a bigger payload capacity; a longer flight time, because there is no need to actuate the airship all the time; a very good stability in the air and no strong oscillations caused by the motors, that can influence the sensors and cameras.

The developed airship is shown in Fig. 1. The length of the airship is 9 m and the maximal diameter of the hull is 2.5 m. The hull volume of 24 m^3 is filled with helium and could lift a payload of about 5-6 kg. The airship is controlled by two 700W synchronous main motors with propellers, which could be vectored, by the tail thruster and the elevator and rudder control surfaces. The operational speed of the airship is up to 30 km/h.

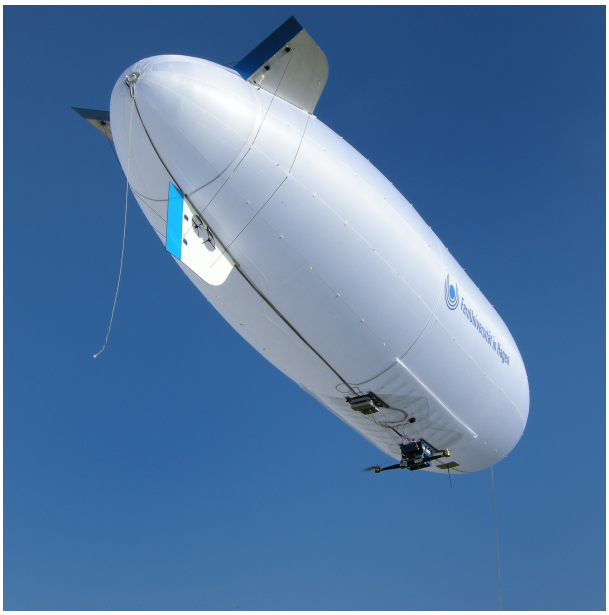

Fig. 1. An autonomous airship of the University of Hagen

2. MATHEMATICAL MODEL OF THE AIRSHIP

For the derivation of the airships mathematical model, two coordinate systems are defined according to Fig. 2. An earth-fixed inertial coordinate system e is used to describe the position and orientation of the airship.

The origin of the body coordinate system b is in the airships centre of volume CV. In this coordinate system, the linear and angular velocities of the airship are described. Moreover, it is used to specify the forces and moments acting on the airships body. The center of gravity CG is the point, in which the total mass of the airship is concentrated (mean location of the gravitational forces).

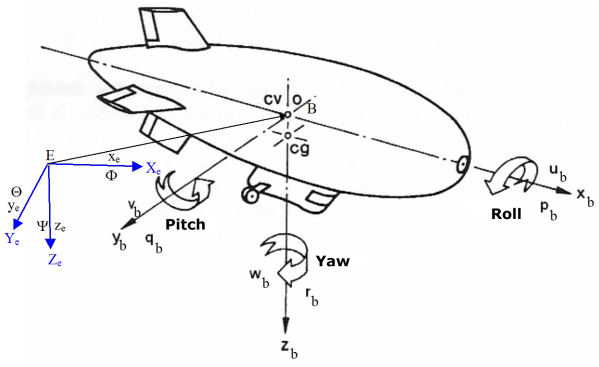

Fig. 2. Coordinate systems of the airship [Khoury (2004)]

2.1 Kinematic model

The kinematic model of the airship involves the position (η_1) and orientation (η_2) vector η, described in the earth-fixed coordinate system e:

$$\eta = {}^{e}\eta = \begin{pmatrix} \eta_1 \\ \eta_2 \end{pmatrix};\ \eta_1 = \begin{pmatrix} x \\ y \\ z \end{pmatrix};\ \eta_2 = \begin{pmatrix} \phi \\ \theta \\ \psi \end{pmatrix} \tag{1}$$

Moreover, ν is the vector of linear (ν_1) and angular (ν_2) velocities

$$\nu = {}^{b}\nu = \begin{pmatrix} \nu_1 \\ \nu_2 \end{pmatrix};\ \nu_1 = \begin{pmatrix} u \\ v \\ w \end{pmatrix};\ \nu_2 = \begin{pmatrix} p \\ q \\ r \end{pmatrix} \tag{2}$$

and τ is the vector of forces (τ_1) and moments (τ_2) acting on the airship.

$$\tau = {}^{b}\tau = \begin{pmatrix} \tau_1 \\ \tau_2 \end{pmatrix};\ \tau_1 = \begin{pmatrix} X \\ Y \\ Z \end{pmatrix};\ \tau_2 = \begin{pmatrix} K \\ M \\ N \end{pmatrix}, \tag{3}$$

where X, Y and Z are forces acting in x-, y- and z-direction and K, M and N are moments acting about these axes. Both are defined in the coordinate system b.

Transformation between the coordinate systems For the transformation of our vector quantities between the coordinate systems, we use the Euler-rotation matrices about the x-, y- and z- axis:

$$R_{x,\phi} = \begin{pmatrix} 1 & 0 & 0 \\ 0 & c_\phi & s_\phi \\ 0 & -s_\phi & c_\phi \end{pmatrix} \tag{4}$$

$$R_{y,\theta} = \begin{pmatrix} c_\theta & 0 & -s_\theta \\ 0 & 1 & 0 \\ s_\theta & 0 & c_\theta \end{pmatrix} \tag{5}$$

$$R_{z,\psi} = \begin{pmatrix} c_\psi & s_\psi & 0 \\ -s_\psi & c_\psi & 0 \\ 0 & 0 & 1 \end{pmatrix} \tag{6}$$

Transformation of translational velocities Using the xyz-convention, we can define a Jacobi-matrix to transform the translational velocities from coordinate system b to e [Fossen (1991)], [Brockhaus (2001)]:

$$J_1(\eta_2) = R^T_{z,\psi} R^T_{y,\theta} R^T_{x,\phi} \tag{7}$$

$$J_1(\eta_2) = \begin{pmatrix} c_\psi c_\theta & -s_\psi c_\phi + c_\psi s_\theta s_\phi & s_\psi s_\phi + c_\psi c_\phi s_\theta \\ s_\psi c_\theta & c_\psi c_\phi + s_\phi s_\theta s_\psi & -c_\psi s_\phi + s_\theta s_\psi s_\phi \\ -s_\theta & c_\theta s_\phi & c_\theta c_\phi \end{pmatrix} \tag{8}$$

The translational velocity applies to:

$$\dot{\eta_1} = J_1(\eta_2)\nu_1 \tag{9}$$

The matrix $J_1(\eta_2)$ is ortogonal ($(J_1(\eta_2)^T J_1(\eta_2) = I$). Therefor the inverse velocity transformation can be written as:

$$\nu_1 = J_1(\eta_2)^{-1}\ \dot{\eta_1} = J_1(\eta_2)^T\ \dot{\eta_1} \tag{10}$$

Transformation of rotational velocities A Jacobi-matrix $J_2(\eta_2)$ is used to transform rotational velocities between the coordinate systems b and e [Brockhaus (2001)].

To transform $\dot{\eta_2}$ from e into the vector ν_2, described in the airships body coordinate system b, following equation must be solved:

$$\nu_2 = \begin{pmatrix} \dot\phi \\ 0 \\ 0 \end{pmatrix} + R_{x,\phi} \begin{pmatrix} 0 \\ \dot\theta \\ 0 \end{pmatrix} + R_{x,\phi} R_{y,\theta} \begin{pmatrix} 0 \\ 0 \\ \dot\psi \end{pmatrix} \tag{11}$$

$$= \begin{pmatrix} 1 & 0 & -s_\theta \\ 0 & c_\phi & s_\phi c_\theta \\ 0 & -s_\phi & c_\phi c_\theta \end{pmatrix} \cdot \begin{pmatrix} \dot\phi \\ \dot\theta \\ \dot\psi \end{pmatrix} \tag{12}$$

$$\nu_2 = J_2^{-1}(\eta_2)\ \dot{\eta_2} \tag{13}$$

The matrix $J_2(\eta_2)$ is not orthogonal ($(J_2(\eta_2)^{-1} \neq J_2(\eta_2)^T$). Solving the equation for $\dot{\eta_2}$ yields to:

$$\dot{\eta_2} = J_2(\eta_2)\ \nu_2 = \begin{pmatrix} 1 & s_\phi t_\theta & c_\phi t_\theta \\ 0 & c_\phi & -s_\phi \\ 0 & s_\phi / c_\theta & c_\phi / c_\theta \end{pmatrix} \cdot \nu_2 \tag{14}$$

Kinematic equations in vector form The kinematic equations can be expressed in a more compact vector form as:

$$\begin{pmatrix} \dot{\eta_1} \\ \dot{\eta_2} \end{pmatrix} = \begin{pmatrix} J_1(\eta_2) & O_{3\times3} \\ O_{3\times3} & J_2(\eta_2) \end{pmatrix} \cdot \begin{pmatrix} \nu_1 \\ \nu_2 \end{pmatrix} \tag{15}$$

$$\dot\eta = J(\eta)\ \nu \tag{16}$$

2.2 Dynamic model

The Newton's laws of linear and angular momentum for rigid bodys (RB) describe the airships dynamic behaviour.

$$M_{RB}\dot\nu + C_{RB}(\nu)\nu = \tau_b \tag{17}$$

The rigid body inertia matrix M_{RB} can be expressed as:

$$M_{RB} = \begin{pmatrix} mI_{3\times3} & -mS(r_G) \\ mS(r_G) & I_b \end{pmatrix} \tag{18}$$

One possible variant to express the rigid body Coriolis- and centrifugal matrix C_{RB} is:

$$C_{RB}(\nu) = \begin{pmatrix} 0_{3\times 3} \\ -mS(\nu_1) + mS(r_G)S(\nu_2) \\ -mS(\nu_1) - mS(\nu_2)S(r_G) \\ -S(I_b\nu_2)) \end{pmatrix} \quad (19)$$

With

- the vector cross product $S(k)$,
- the inertia tensor I_b,
- the mass of the airship m and
- the position of the center of mass ${}^b r_G$.

The vector τ_b of external forces and moments can be written as

$$\tau_b = \tau_{add} + \tau_V + \tau_{rest} + \tau_{FK} + \tau_{Fin} + \tau_A \quad (20)$$

where the parts of τ_b are:

- added -mass and -Coriolis and centripedal matrix $\tau_{add} = -M_A\dot{\nu_r} - C_A(\nu_r)\nu_r$
- damping forces of fuselage $\tau_V = -D(\nu_r)\nu_r$
- restoring forces $\tau_{rest} = -g(\eta)$
- Froude-Krylov forces $\tau_{FK} = M_{FK}\dot{\nu_c}$
- fixed fins and control surfaces $\tau_{Fin} = D_{Fin}(\nu_r, \delta) - D_{Fin}(\nu_r)$
- propulsive forces $\tau_p = P_S + P_B + P_{Stern}$

ν_r is the relative airspeed.

Added -mass and -Coriolis and centripedal matrix A body accelerates a certain surrounding air mass with movement. The body behaves thereby simplified, as if an additional mass would be adhere to it. For a completely in a medium submerged body with three planes of symmetry and low velocity, the added mass- M_A and the added Coriolis and centripedal- matrix $C_A(\nu_r)$ can therefore be considered:

$$M_A = diag(X_{\dot{u}}, Y_{\dot{v}}, Z_{\dot{w}}, K_{\dot{p}}, M_{\dot{q}}, N_{\dot{r}}) \quad (21)$$

$$C_A(\nu_r) = \quad (22)$$
$$\begin{pmatrix} 0 & 0 & 0 & 0 & Z_{\dot{w}}w_r & -Y_{\dot{v}}v_r \\ 0 & 0 & 0 & -Z_{\dot{w}}w_r & 0 & X_{\dot{u}}u_r \\ 0 & 0 & 0 & Y_{\dot{v}}v_r & -X_{\dot{u}}u_r & 0 \\ 0 & Z_{\dot{w}}w_r & -Y_{\dot{v}}v_r & 0 & N_{\dot{r}}r_r & -M_{\dot{q}}q_r \\ -Z_{\dot{w}}w_r & 0 & X_{\dot{u}}u_r & -N_{\dot{r}}r_r & 0 & K_{\dot{p}}p_r \\ Y_{\dot{v}}v_r & -X_{\dot{u}}u_r & 0 & M_{\dot{q}}q_r & -K_{\dot{p}}p_r & 0 \end{pmatrix}$$

For example: The force Y_A along the y axis due to an acceleration $\dot{v}$ in y-direction is:

$$Y_A = Y_{\dot{v}}\dot{v} \quad mit \quad Y_{\dot{v}} = \frac{\partial Y}{\partial \dot{v}} \quad (23)$$

Damping forces of fuselage The damping effects on the airships fuselage are mainly caused by linear and quadratic surface frictions, due to laminar and turbulent fluid motions. For a completely submerged body, the linear and quadratic damping forces can simplyfied be written:

$$\begin{aligned} &D(\nu_r) = diag(X_u, Y_v, Z_w, K_p, M_q, N_r) \\ &+diag(X_{u|u|}|u_r|, Y_{v|v|}|v_r|, Z_{w|w|}|w_r|, \\ &K_{p|p|}|p_r|, M_{q|q|}|q_r|, N_{r|r|}|r_r|) \end{aligned} \quad (24)$$

Restoring forces The gravitational force $W = mg$ works against the buoyancy force $B = g\rho V$.

$$f_G = J_1^{-1}(\eta_2)\begin{pmatrix} 0 \\ 0 \\ W \end{pmatrix};\ f_B = -J_1^{-1}(\eta_2)\begin{pmatrix} 0 \\ 0 \\ B \end{pmatrix} \quad (25)$$

The restoring forces can be therefore represented by:

$$g(\eta) = -\begin{pmatrix} f_G(\eta_2) + f_B(\eta_2) \\ r_G \times f_G(\eta_2) + r_B \times f_B(\eta_2) \end{pmatrix} \quad (26)$$

${}^b r_B$ is the position of the center of buoyancy.

Froude-Krylov forces The Froude-Krylov forces results from differences of pressure, acting on the body surface due to the flow rate v_c of the surrounding air masses. The Froude-Krylov forces can be expressed as:

$$\tau_{FK} = M_{FK}\dot{\nu_c} \quad (27)$$

M_{FK} can be calculated with der inertia tensor and the mass of the displaced air. Assuming a buoyancy neutral airship and homogeneous mass distribution, the inerta matrix M_{FK} could be set equal to M_{RB}.

Fixed fins and control surfaces The airship has three by 120 degrees displaced stabilisation fins with control surfaces. Each fin has its own coordinate system f_i, whose x_i- direction is equal to the bodies x-direction. The control surfaces can be rotated about an angle δ_i around its y_i-axis. [Campa and Innocenti (1999)] The rotation matrix ${}^b R_{fi}$ transforms the fin forces from coordinate system f_i to b.

$${}^b R_{f_i} = R^{-1}_{x,(\pi/2+2\pi k/3)} R^{-1}_{y,\delta_i} \quad (k = 0, 1, 2) \quad (28)$$

δ_i is null for all fixed stabilisation fins. The velocity of fin i in relation to the wind flow, denoted in coordinate system b, can be written:

$${}^b V_{Fi/c} = ({}^b V_{b/c} + {}^b w_{b/c} \times {}^b P_{Fi}) \quad (29)$$

${}^b P_{Fi}$ is the position of the i-te fin. ${}^b w_{b/c}$ is the angular- and ${}^b V_{b/c}$ the translational- velocity part of the relativ airspeed ν_r.

${}^b V_{Fi/c}$ can be transformed into the fin coordinate system f_i as follows:

$${}^{fi} V_{Fi/c} = {}^{fi} R_b \, {}^b V_{Fi/c} \quad (30)$$

The wind in y-direction of f_i leads to no application of force and can therefore be neglected. The angle of attack α_{fi} between the wind- and the fin coordinate system is given through:

$$\alpha_{fi} = atan2({}^{fi} V_{Fi/c}(z), {}^{fi} V_{Fi/c}(x)) \quad (31)$$

The positive x- axis of the wind w coordinate system shows toward the relative velocity between fin and wind-current. A transformation from the wind into the fin coordinate system can be achieved with the matrix:

$$ {}^{fi}R_w = \begin{pmatrix} c_{\alpha_{fi}} & 0 & -s_{\alpha_{fi}} \\ 0 & 1 & 0 \\ s_{\alpha_{fi}} & 0 & c_{\alpha_{fi}} \end{pmatrix} \quad (32) $$

Damping forces of fins are given in the wind coordinate system:

$$ {}^{w}F_{Fi} = -\frac{1}{2}\rho A \begin{pmatrix} C_D \\ C_C \\ C_L \end{pmatrix} {}^{fi}V_{Fi/c}^{T} \, {}^{fi}V_{Fi/c} \quad (33) $$

C_D, C_C and C_L are aerodynamic damping coefficients.

The forces are transformed from w into the b coordinate system:

$$ {}^{b}F_{Fi} = {}^{b}R_{fi} \, {}^{fi}R_w \, {}^{w}F_{Fi} \quad (34) $$

and leads to moments via the lever arm ${}^{b}P_{Fi}$:

$$ {}^{b}M_{Fi/b} = {}^{b}P_{Fi} \times {}^{b}F_{Fi} \quad (35) $$

τ_{Fin} can be devided into forces and moments caused by the stabilisation fins $D_{Fin}(\nu_r)$ and the control surfaces $-D_{Fin}(\nu_r, \delta)$.

$$ \tau_{Fin} = -D_{Fin}(v_r, \delta) + D_{Fin}(\nu_r) \quad (36) $$
$$ = \sum_{i=1}^{4} \begin{pmatrix} {}^{b}F_{Fi}(v_r, \delta) \\ {}^{b}M_{Fi/b}(v_r, \delta) \end{pmatrix} + \sum_{i=1}^{4} \begin{pmatrix} {}^{b}F_{Fi}(v_r) \\ {}^{b}M_{Fi/b}(v_r) \end{pmatrix} $$

Propulsive forces The airship is actuated by two main gondola motors with propellers, witch could be vectored (rotated about an angle α around the bodys y-axis). The motor forces ${}^{a}F_S$ and ${}^{a}F_B$ points in x-direction from coordinate system a. The rotation matrix ${}^{b}R_a$ transforms the motor forces from coordinate system a to b.

$$ {}^{b}R_a = R_{y,\alpha} \quad (37) $$

$$ {}^{b}F_S = {}^{b}R_a \, {}^{a}F_S; \quad {}^{b}F_B = {}^{b}R_a \, {}^{a}F_B \quad (38) $$

The main gondula motor forces and moments can be written as:

$$ P_S = \begin{pmatrix} {}^{b}F_S \\ {}^{b}r_S \times {}^{b}F_S \end{pmatrix}; \; P_B = \begin{pmatrix} {}^{b}F_B \\ {}^{b}r_B \times {}^{b}F_B \end{pmatrix} \quad (39) $$

${}^{b}r_S$ and ${}^{b}r_B$ are the positions of the main gondula propellers.

The tail motor forces and moments acting upon the airship can be written as:

$$ P_{Stern} = \begin{pmatrix} F_{Stern} \\ r_{Stern} \times F_{Stern} \end{pmatrix} \quad (40) $$

F_{Stern} and ${}^{b}r_{Stern}$ are the tail motor force and its position.

Wind current The wind current points towards the x-axis of w. One can transform the wind current from w into the e coordinate system, by rotating about the angle of attack α_c and the angle of sideslip β_c:

$$ {}^{e}V_c = R_{y,\alpha_c} R_{z,-\beta_c} \cdot {}^{w}V_c \quad (41) $$

The transformation in the body coordinate system can be achieved with $J(\eta)$. The relative speed $\nu_r = \nu - \nu_c$ is the speed between the airship (ν) and the wind velocity (ν_c).

2.3 The overall airchip model

The overall non-linear 6-DOF (degrees of freedom) model of the airship has the following form:

$$ \begin{aligned} &(M_{RB} + M_A)\dot{\nu_r} + C_{RB}(\nu)\nu + C_A(\nu_r)\nu_r \quad (42) \\ &+D(\nu_r)\nu_r + D_{Fin}(\nu_r) + g(\eta) = \tau_P + D_{Fin}(\nu_r, \delta) \\ &\dot{\eta} = J(\eta) \; \nu \end{aligned} $$

3. DESING OF THE AIRSHIP CONTROL

A very good solution to handle all input/output variables is to use a state-space controller. The airship is a non-linear system. Therefore, we decided to use a nonlinear gain-scheduling controller. A gain-scheduling controller optimizes the linear state-space controller parameters to various operating points of the airship. There exists many design methods for linear state controllers. We choose an LQR-based controller design, because of its relatively easy implementation. However, LQR-controller designs are only applicable for linear systems. Therefore, in a first step, the linearization of the airship model is necessary. It is reasonable to split the linearized model of the whole airship into a lateral and a longitudinal subsystem. Each of them are used to control some particularly motions. The control-loop structures for lateral and longitudinal motions are explained bellow. Moreover, the airship is a nonholonomic 6-DOF system. So, it is not possible to control it in every direction with arbitrary orientation. The following control system is at this time only designed without implementing the tail fin control surfaces as controller inputs.

3.1 Linearisation of the airship model

Equilibrium points The nonlinear airship system can be writtes as:

$$ \dot{x}(t) = f(x(t), u(t)) \quad (43) $$

An equilibrium point corresponds to a condition, at which the dynamical system is in steady state.

$$ 0 = \dot{x}_0 = f(x_0, u_0) \quad (44) $$

Due to the complex aerodynamic data, the equilibrium points cannot be found analytically. We use a numeric optimization algorithm to find the equilibrium points x_0, u_0 over the flight envelope. Therefor, a convex cost function is minimized.

$$ \begin{aligned} F = \min = {} & \dot{u_0}^2 + \dot{v_0}^2 + \dot{w_0}^2 + \dot{p_0}^2 + \dot{q_0}^2 + \dot{r_0}^2 + \\ & (\dot{x_0} - V_{GS})^2 + \dot{y_0}^2 + \dot{z_0}^2 + \dot{\phi_0}^2 + \dot{\theta_0}^2 + \dot{\psi_0}^2 + \quad (45) \\ & v_0^2 + p_0^2 + q_0^2 + r_0^2 + x_0^2 + y_0^2 + z_0^2 + \phi_0^2 + \psi_0^2 \end{aligned} $$

The scheduling-variable V_{GS} specifies various speeds of the airship in $\dot{x_0}$ direction and so the flight envelope.

Linaerization With the derivations

$$ \widetilde{x} = x - x_0 \quad \widetilde{u} = u - u_0 \quad (46) $$

the system can be lineaized by using a multivariable Taylor serie.

$$\dot{\tilde{x}}(t) \approx \left.\frac{\partial f}{\partial x}\right|_{x=x_0;u=u_0} \widetilde{x} + \left.\frac{\partial f}{\partial u}\right|_{x=x_0;u=u_0} \widetilde{u} \qquad (47)$$

Were $A = \left.\frac{\partial f}{\partial x}\right|_{x=x_0;u=u_0}$ and $B = \left.\frac{\partial f}{\partial u}\right|_{x=x_0;u=u_0}$ are the $n \times n$ and $n \times m$ Jacobi-matrices.

Because of the complex nonlinear data (aerodynamic data), the linearization cannot be done analytically. The numerical linearization can be done by perturbing each state or input signal slightly from its equilibrium points. The matrices A (and B) can be approximated as:

$$\dot{\tilde{x}}_1 - \dot{\tilde{x}}_{-1} = f(x_0) + h \left.\frac{\partial f}{\partial x}\right|_{x=x_0} - f(x_0) + h \left.\frac{\partial f}{\partial x}\right|_{x=x_0} \qquad (48)$$

$$A = \left.\frac{\partial f}{\partial x}\right|_{x=x_0} \approx \frac{\dot{\tilde{x}}_1 - \dot{\tilde{x}}_{-1}}{2h} \qquad (49)$$

The linear model of the airship can be expressed in a well-known general state-space form:

$$\dot{\widetilde{x}} = A\widetilde{x} + B\widetilde{u} \qquad (50)$$

$$y = C\widetilde{x} + D\widetilde{u} \qquad (51)$$

$$C = I_{(12\times 12)} \qquad (52)$$

$$D = 0_{(12\times 3)} \qquad (53)$$

3.2 Lateral controller

The heading system is nonholonomic, because the yaw angle can not be controlled without changing the airships y position. The main purpose of the lateral system is to control the yaw angle ψ. For this reason, the y position is not included in the state vector: $xH = v, p, r, \phi, \psi$. The input variable is $u = F_{Stern}$. [Metelo and Campos (2003)]

The state and input matrices for the lateral sub-system are extracted from the linearised model by using the new state vector x_H:

$$A_H = \begin{array}{c} \begin{matrix} v & p & r & \phi & \psi \end{matrix} \\ \begin{pmatrix} a_{2,2} & a_{2,4} & a_{2,6} & a_{2,10} & a_{2,12} \\ a_{4,2} & a_{4,4} & a_{4,6} & a_{4,10} & a_{4,12} \\ a_{6,2} & a_{6,4} & a_{6,6} & a_{6,10} & a_{6,12} \\ a_{10,2} & a_{10,4} & a_{10,6} & a_{10,10} & a_{10,12} \\ a_{12,2} & a_{12,4} & a_{12,6} & a_{12,10} & a_{12,12} \end{pmatrix} \end{array} \begin{matrix} v \\ p \\ r \\ \phi \\ \psi \end{matrix} \qquad (54)$$

$$B_H = \begin{array}{c} F_{Stern} \\ \begin{pmatrix} b_{2,1} \\ b_{4,1} \\ b_{6,1} \\ b_{10,1} \\ b_{12,1} \end{pmatrix} \end{array} \begin{matrix} v \\ p \\ r \\ \phi \\ \psi \end{matrix} \qquad (55)$$

The state vector deviation from the operating point is given by:

$$\tilde{x}_H = x_H - x_{H_{d(0)}} = \begin{pmatrix} v - v_0 \\ p - p_0 \\ r - r_0 \\ \phi - \phi_0 \\ \psi - \psi_0 - (\psi_d - \psi_0) \end{pmatrix} \qquad (56)$$

The controlled input variable

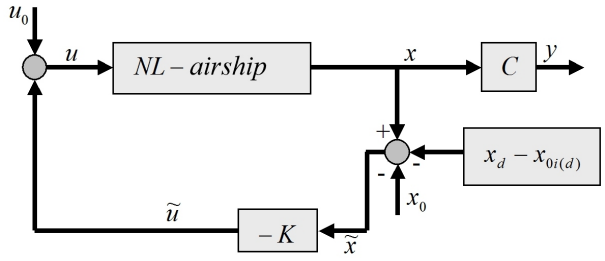

Fig. 3. Closed-loop lateral system

$$\tilde{u}_H = -K_H \tilde{x}_H \qquad (57)$$

stabilizes the state space equation of the lateral system:

$$\dot{x}_H = A_H \tilde{x}_H + B_H \tilde{u}_H \qquad (58)$$

In order to find the optimal controller parameters, the quadratic cost criterion should be minimized:

$$J = \frac{1}{2} \int_0^\infty \left[x^T(t) Q x(t) + u^T(t) R u(t) \right] dt = \min_K \qquad (59)$$

Therefore, the optimal controller parameters K can be calculated by solving the Riccati equation for the matrix P:

$$PA + A^T P - PBR^{-1}BP + Q = 0 \qquad (60)$$

$$K = R^{-1} B^T P \qquad (61)$$

The parameters $q_i > 0$ from the weight matrix $Q = diag(q_1, q_2, \ldots, q_n)$ are weighting the associated states. The parameters $r_i > 0$ from the weight matrix $R = diag(r_1, r_2, \ldots, r_m)$ are weighting the associated inputs.

The closed-loop lateral system with state controller is shown in Fig. 3.

All poles of the open-loop lateral system are stable. However, one of them is on the imaginary axis. The pole location of the open-loop lateral system is shown is Fig. 4.

The weighting matrices $Q = Q^T \geq 0$ with $n = 5$ and $R = R^T \geq 0$ with $m = 1$ elements on the main diagonal should be selected in such a way, to ensure, that the output variable F_{Stern} does not saturate. Moreover, the state variable $(\psi - \psi_d)$ should converges faster to zero as the others. This request can be realised through a larger value for q_5 in the weighting matrix Q.

Resulting poles of the closed-loop heading system with LQR-controller are shown in Fig. 5. The step response for the yaw angle is shown in Fig. 6.

3.3 Longitudinal controller

The longitudinal (XZ) control is dedicated to control the state variables u and z. The gondola drives with propellers are used as input variables. Similar to the lateral system, the longitudinal system is not independent controllable in all DOF. The yaw angle ψ affects the controllability of

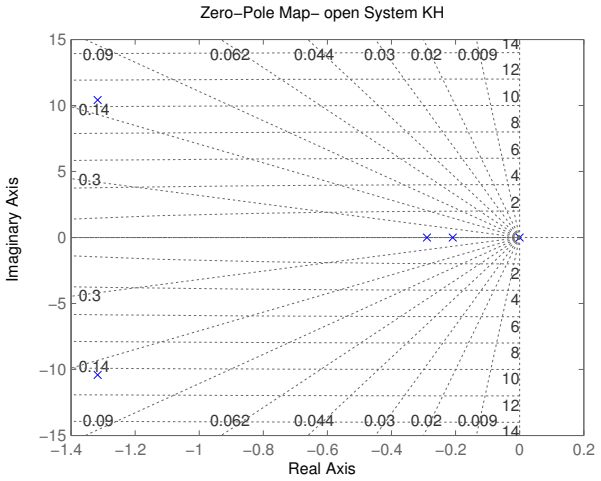

Fig. 4. Poles of the open-loop lateral system

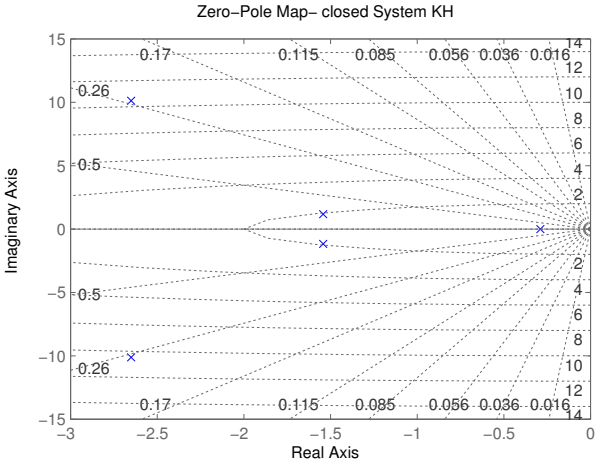

Fig. 5. Poles of the closed-loop lateral system

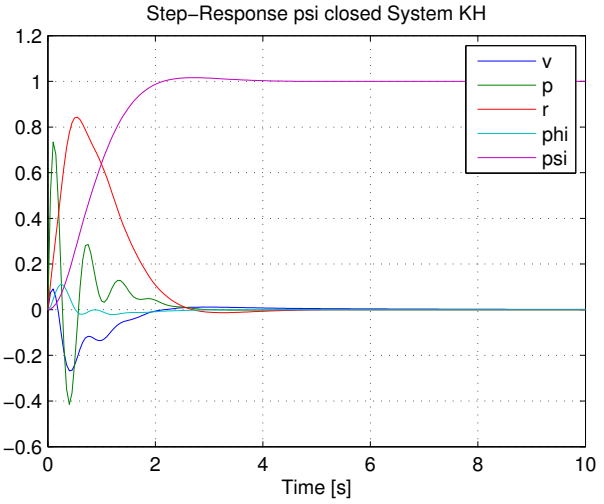

Fig. 6. Step response (yaw angle) of the lateral system

the $x-$position of the airship. Therefore, the state variable x is not included in state vector for longitudinal control. Moreover, the pitch angle θ is at the equilibrium points not equal to zero. Thus, it is not reasonable to control this angle to zero. Therefore, this variable is also not included in the resulting state vector $x_{XZ} = u, w, q, z$. The input vector includes the forces, generated by the main propellers. The input forces $F(\alpha)$ are splitted for control purpose in an x and z direction $u = F_x, F_z$. [Metelo and Campos (2003)]

$$F = FS + FB \tag{62}$$

$$F_x = Fcos(\alpha) \tag{63}$$

$$F_z = Fsin(\alpha) \tag{64}$$

The linearized longitudinal state and input matrices are:

$$A_{XZ} = \begin{array}{c} \begin{matrix} u & w & q & z \end{matrix} \\ \begin{pmatrix} a_{1,1} & a_{1,3} & a_{1,5} & a_{1,9} \\ a_{3,1} & a_{3,3} & a_{3,5} & a_{3,9} \\ a_{5,1} & a_{5,3} & a_{5,5} & a_{5,9} \\ a_{9,1} & a_{9,3} & a_{9,5} & a_{9,9} \end{pmatrix} \end{array} \begin{matrix} u \\ w \\ q \\ z \end{matrix} \tag{65}$$

and

$$B_{XZ} = \begin{array}{c} \begin{matrix} F_x & F_z \end{matrix} \\ \begin{pmatrix} b_{1,2} & b_{1,3} \\ b_{3,2} & b_{3,3} \\ b_{5,2} & b_{5,3} \\ b_{9,2} & b_{9,3} \end{pmatrix} \end{array} \begin{matrix} u \\ w \\ q \\ z \end{matrix} \tag{66}$$

The primary controlled variables u and v are coupled, because the flight speed u can affect the altitude z. Since the LQR-controller has only proportional feedback, there will result a not negligible error. By introducing an I-type feedback, this error can be eliminated. For this purpose, new state variables are defined:

$$x_{\int} = (x_{\int u}, x_{\int z}) = \left(\int_0^t u(\tau)d\tau, \int_0^t z(\tau)d\tau \right) \tag{67}$$

The new state variables can be added to the existing longitudinal state-space variables,

$$\tilde{x}_{XZ} = x_{XZ} - x_{XZ_{d(0)}} = \begin{pmatrix} u - u_0 - (u_d - u_0) \\ w - w_0 \\ q - q_0 \\ z - z_0 - (z_d - z_0) \end{pmatrix} \tag{68}$$

witch results in the following controlled longitudinal overall system:

$$\begin{pmatrix} \dot{\tilde{x}}_{XZ} \\ \dot{\tilde{x}}_{\int u} \\ \dot{\tilde{x}}_{\int z} \end{pmatrix} = \begin{pmatrix} A_{XZ} & 0_{4\times 2} \\ \begin{pmatrix} 1 & 0 & 0 & 0 \\ 0 & 0 & 0 & 1 \end{pmatrix} & 0_{2\times 2} \end{pmatrix} \begin{pmatrix} \tilde{x}_{XZ} \\ \tilde{x}_{\int u} \\ \tilde{x}_{\int z} \end{pmatrix} + \begin{pmatrix} B_{XZ} \\ 0_{1\times 2} \\ 0_{1\times 2} \end{pmatrix} \tilde{u}_{XZ} \tag{69}$$

The input signals are calculated as:

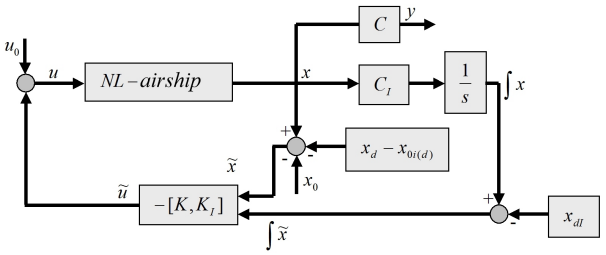

Fig. 7. Closed-loop longitudinal system with additive I-controller

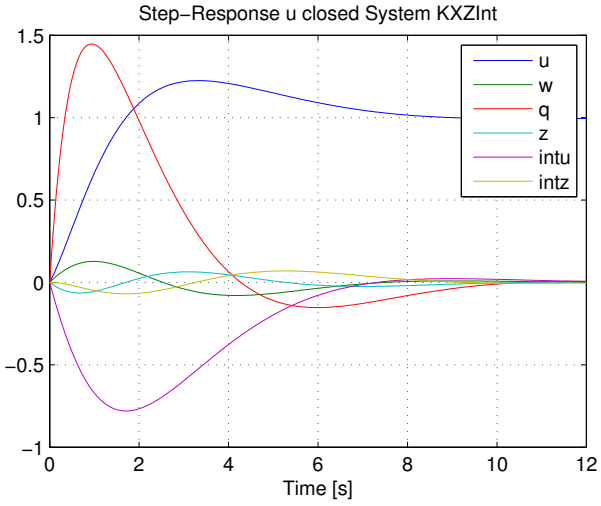

Fig. 8. Step response of the longitudinal system

$$\tilde{u}_{XZ} = -\begin{pmatrix} K & K_{\int u} & K_{\int z} \end{pmatrix} \begin{pmatrix} \tilde{x}_{XZ} \\ \tilde{x}_{\int u} \\ \tilde{x}_{\int z} \end{pmatrix} \tag{70}$$

Fig. 7 shows the closed-loop longitudinal system.

The procedure for calculating the controller parameters is similar to the lateral system. In this case, the state variables $u-ud, z-zd, x_{\int u}$ and $x_{\int z}$ should be controlled faster than the others. Therefore, the weighting coefficients $q1, q4, q5$ and $q6$ of the matrix Q must be greater then the values of $q2$ and $q3$, respectively. The resulting LQR-controller is a 2×6 matrix.

The values of integral-feedback gains can reach very large values, if the airship has an unilateral error from the desired flight path. Therefore, it is necessary to implement an anti-wind-up saturation of these signals.

The step response of the longitudinal closed-loop system for the output variable u is shown in Fig. 8.

3.4 Gain-scheduling controller

A linear controller can only guarantee stability in a short range about the operating point, for which it was designed. However, the airship should be controlled under all possible flight conditions. This can be realised by using a nonlinear controller.

A nonlinear gain-scheduling controller acts as a switch between a lot of linear controllers. Each of them are

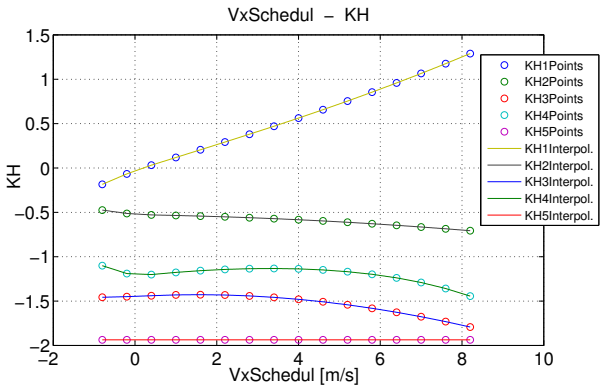

Fig. 9. Parameters of the LQR-controller for lateral system

designed for a specific operating point. Operating points are equilibrium points for a certain value of the gain-scheduling variable s [Moutinho (2007)].

$$0 = f(x_0(s), u_0(s)) \tag{71}$$

The gain-scheduling variable s for the airship is defined by its speed. This speed corresponds to the x-velocity ${}^{exy}v_{rx}$ of the relative speed v_r, transformed into XY plane of the earth coordinate system:

$${}^{exy}v_r = \begin{pmatrix} {}^{exy}v_{rx} \\ {}^{exy}v_{ry} \\ {}^{exy}v_{rz} \end{pmatrix} = J_1(\phi, \theta, 0) \cdot v_r \tag{72}$$

The nonlinear airship model $\dot{x} = f(x, u)$ is linearized at all equilibrium points (Eq. 71.), given by various values $s(1), s(2), ...s(n)$ of the gain-scheduling variable s.

In this way, n linear systems are developed:

$$\dot{\tilde{x}} = A(s)\tilde{x} + B(s)\tilde{u} \tag{73}$$

$$\tilde{y} = C(s)\tilde{x} \tag{74}$$

For each of the n linear systems, an LQR controllers $K(s)$ will be calculated:

$$\tilde{u} = -K(s)\tilde{x} \tag{75}$$

The controller parameters $K(s)$ are then interpolated between all equilibrium points. The interpolated controller parameters $K(s)$ are depending on the value of the gain-scheduling variable s.

The graphs in Fig. 9. shows the calculated and interpolated parameters of the LQR-controller for the lateral control system.

It is easy to detect that there are some step changes in the parameter values. These can lead to an instability of the whole closed-loop system, if it is controlled between two operating points with big changes in controller parameters. As a solution we designed a checking algorithm, which allows only to change the coefficients of controller parameters with limited range and so without step changes in the scheduled controller coefficients. The step changes of the controller coefficients are detected by using the derivation of the controller coefficients curve. The following figure

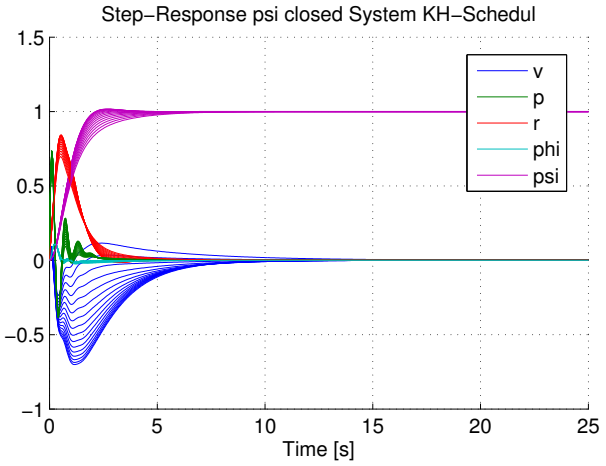

Fig. 10. Step response of the gain-scheduled controlled lateral system

Fig. 10. shows the step responses of the designed lateral gain-scheduling controller.

3.5 Navigation

The above described lateral and longitudinal control systems are not able to control the airship in all 6DOF, as it is a nonholonomic and so a not fully controllable system. Besides the yaw angle ψ, it must be also controlled the altitude Z_e and the speed u in X_b-direction. For flying on an appropriate flight trajectory, the desired set values must be proper generated for the controllers.

For this purpose we designed a navigation module, which switches between the two operating modes of the airship - steady state control and point-to-point flight. The point-to-point control is used to flight to a new target point. In this mode, the lateral control system is used for adjusting the airship orientation towards the desired set position. The longitudinal system controls the desired speed u and desired Z_e position of the airship. The desired speed u is increased, if the control deviation of the orientation decreases. If the airship is nearby the target point, the steady state control mode is activated. In this mode, the maximal speed of the airship is limited and decreases with decreasing distance to the target point. This strategy prevents the airship to do very ineffective maneuvers in the neighbourhood of the set position. Moreover, the airship can flight backward to the target position in this mode [Metelo and Campos (2003)].

Combining these strategies yields to a complex motion control for the airship. Fig. 11. shows simulation results of a typical airship flight with take-off, movement on a linear and circular composed trajectory with constant altitude and landing [Moutinho (2007)].

4. CONCLUSION

In this paper we presented the design procedure for a gain-scheduled LQR controller for an autonomous airship. Two types of control sub-systems (lateral, longitudinal) have been designed from the nonlinear 6DOF airship model to fulfill different goals (yaw as well as speed and position control). The navigation system generates

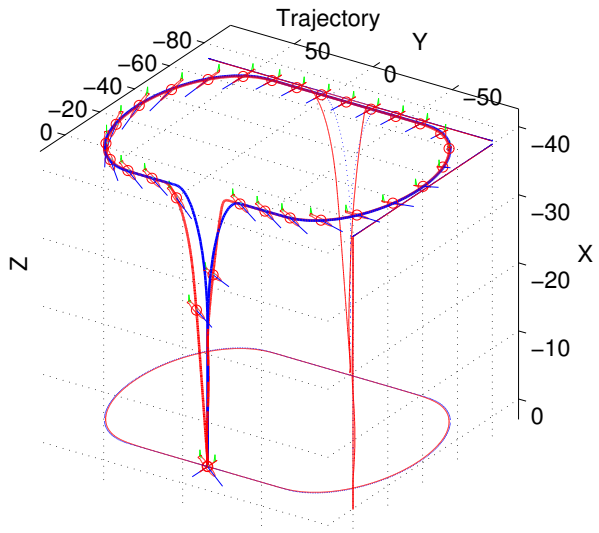

Fig. 11. Spline trajectory with gain-scheduled LQR-controller

appropriate inputs for the controllers of both sub-systems and combines them to a complex control unit, witch allows the airship to follow an adequate flight trajectory. Simulations shows a good performance of the designed control system, which will be tested on the real airship in near future.

REFERENCES

Brockhaus (2001). *Flugregelung*. Springer, Berlin, 2 edition.

Campa, G. and Innocenti, M. (1999). Model of an underwater vehicle (shark.pdf). University of Pisa, 56126 Pisa, Italy, Department of Electrical Systems and Automation. URL `http://www.mathworks.com/matlabcentral/fileexchange/1207`.

Fossen, T.I. (1991). *Nonlinear Modelling and Control of Underwater Vehicles*. Ph.D. thesis, Norwegian Institute of Technology, Department of Marine Technology.

Jaimes, A., Kota, S., and Gomez, J. (2008). An approach to surveillance an area using swarm of fixed wing and quad-rotor unmanned aerial vehicles uav(s). In *IEEE International Conference on System of Systems Engineering*.

Khoury, G. (2004). *Airship Technology (Cambridge Aerospace)*. Cambridge Univ Press, 1 edition.

Metelo, F.M.S. and Campos, L.R.G. (2003). Vision based control of an autonomous blimp (videoblimp). URL `http://www.isr.ist.utl.pt/vislab/thesis/03-videoblimp-tfc.pdf`.

Moutinho, A.B. (2007). *Modelling and Nonlinear Control for Airship Autonomous Flight*. Ph.D. thesis, UNIVERSIDADE TÉCNICA DE LISBOA, INSTITUTO SUPERIOR TÉCNICO.

Prior, S.D., Shen, S.T., Karamanoglu, M., Odedra, S., Erbil, M.A., Barlow, C., and Lewis, D. (2009). The future of battlefield micro air vehicle systems. In *International Conference on Manufacturing and Engineering Systems, Huwei, Taiwan*.